

ROSAT coronal temperatures of young late type stars

Thomas Preibisch

Astronomisches Institut der Universität Würzburg, Am Hubland, D-97074 Würzburg, Germany (preib@astro.uni-wuerzburg.de)

Received 9 April 1996 / Accepted 15 July 1996

Abstract. We analyze ROSAT X-ray spectra of a sample of young late type stars by fitting them with a continuous emission measure model with power-law temperature dependence up to a maximum temperature. This model gives successful fits to all spectra of our sample. While most of the spectra can also be fitted equally successfully with the frequently used two temperature model, we argue and provide evidence that the continuous temperature distribution model probably describes the coronal temperature structure in a more meaningful way.

From our fitting results we find a very good correlation between the X-ray surface flux and the maximum coronal temperature with the functional form $F_X \propto T_{\max}^{(2.2 \pm 0.2)}$. This correlation extends over several orders of magnitude and is valid for the very young T Tauri stars as well as for the much older young main sequence stars in our sample. Since the X-ray surface flux is a good measure of the stellar activity and shows a clear dependence on the stellar rotational velocity, the correlation means that the coronal temperature is related to the X-ray activity and ultimately determined by stellar rotation.

Finally, we interpret our results with a simple analytic loop model and find that the coronae of the active young stars are probably dominated by loops with generally higher pressure as compared to typical solar active region loops.

Key words: X-rays: stars – stars: pre-main-sequence – stars: coronae

1. Introduction

The X-ray observations of the ROSAT satellite (see Trümper 1983) provide the largest database to date for an X-ray study of stellar coronae. Most recent investigations have dealt mainly with the amplitude of the X-ray emission and its dependence on basic stellar parameters (see e.g. Fleming et al. 1995; Schmitt et al. 1995). In this study we will focus our interest on the analysis of the X-ray spectra and the determination of the coronal temperature structure.

A similar study has been performed by Schmitt et al. (1990), using X-ray spectra obtained with the IPC detector on board of the EINSTEIN observatory. The ROSAT data, however, offer

considerable advantages over the EINSTEIN data: First, the spectral resolution of the ROSAT Positional Sensitive Proportional Counter PSPC ($\Delta E/E \approx 40\%$ at 1 keV; see Pfeffermann et al. 1987), is significantly higher as compared to that of the EINSTEIN IPC ($\Delta E/E \approx 100\%$). Second, much more late type stars have been observed in deep ROSAT pointings than in EINSTEIN observations.

We are aware that the amount of information that can be inferred from the moderate resolution PSPC spectra is quite limited and observations with higher spectral resolution would allow a much more detailed study of the coronal temperature structure. However, the handful of stars for which high resolution X-ray spectra were taken e.g. with the EINSTEIN Focal Plane Crystal Spectrometer or the EXOSAT transmission grating are much too few to derive general stellar spectral properties. In the last years, the EUVE satellite (see Bowyer & Malina 1991) has performed high resolution extreme-ultraviolet observations of several late type stars. The EUVE data are well suited for a determination of the coronal temperature distribution (for a review see Drake 1996), but unfortunately the number of observed stars again is very small. Thus, only the ROSAT data allow one to study a reasonably large sample of late type stars. However, we will keep in mind the EUVE results and refer to them whenever needed.

We will restrict our study to late type stars (spectral type between F and M), since for this class of stars a coronal origin of the X-ray emission is well established (see Pallavicini 1989). The ages of the stars in our sample range from $\lesssim 10^6$ years for the T Tauri stars (TTS) up to the age of the Sun ($\approx 5 \times 10^9$ years). To explain the motivation of this study, one just has to compare the X-ray properties of TTS (for a recent review see Montmerle et al. 1993) to those of the Sun: Most TTS are vigorous X-ray emitters with X-ray luminosities of up to $L_X \gtrsim 10^{31}$ erg/sec, which exceeds the solar level by about three orders of magnitude; furthermore, for many TTS the coronal temperatures inferred from the X-ray spectra are very high, $T \gtrsim 10^{7.5}$ K, as compared to typical solar coronal temperatures of just a few 10^6 K. It has to be noted that the high levels of X-ray emission can not at all be simply explained by the higher coronal temperatures: since the radiative cooling function of the coronal plasma decreases for temperatures between 10^6 K and $\approx 10^{7.5}$ K (cf. Fig. 1 in Bruner & McWhirter 1988), a higher coronal tempera-

ture takes even more emission measure to produce the required level of emission.

One of the questions we want to address is, whether the coronal properties are a function of age. Another point we will investigate is, what change in condition from the Sun can produce the high X-ray luminosities and coronal temperatures. We are especially interested in what determines the coronal temperatures.

Young stars are also known to show very powerful X-ray flares with a total energy output exceeding that of large solar flares by up to 5 orders of magnitude (e.g. Montmerle et al. 1983; Preibisch et al. 1993, 1995). In this study we explicitly exclude X-ray flares, since we want to study the quiescent corona (for an overview on X-ray flares on young stars see e.g. Preibisch & Neuhäuser 1995).

2. Sample stars and X-ray data analysis

For this study we have used archive data from 24 deep ROSAT PSPC observations of young clusters or individual stars. We extracted X-ray spectra of TTS from ROSAT observations of the Orion Nebula, the ρ Oph star forming region, and the Cha I dark cloud. X-ray spectra of young main-sequence stars were obtained from archive data of the young cluster IC2391, the Pleiades, and the Hyades. In order to fill the gap between the age of the Hyades and the Sun, we also analyzed archive data on 8 field stars, originally collected by Dorren & Guinan (1994) as a sample of very good solar proxies with different ages and rotational velocities (see also Dorren et al. 1995; Güdel et al. 1996a,b). Basic information on the data sets used in our study is summarized in Table 1. In Table 2 we give spectral type, stellar radius, and rotational properties of the sample stars. The entry “bin” in the last column means that the star is known as a binary, “bin?” means that binarity is suspected. “C” is the abbreviation for “classical T Tauri star”, defined as showing H α in emission with $W(\text{H}\alpha) \geq 10 \text{ \AA}$, “W” that for “weak line T Tauri star” ($W(\text{H}\alpha) < 10 \text{ \AA}$). The data have been collected from the references given in Table 1 and additionally from Gagné & Caillault (1994), Gagné et al. (1995b), Hempelmann et al. (1995), Herbig & Bell (1988), Huenemoerder et al. (1994), Micela et al. (1990), and Prosser et al. (1995).

All X-ray data were retrieved from the ROSAT data archive at MPE. The data analysis was performed with the EXSAS software package (Zimmermann et al. 1993). We extracted X-ray spectra for all sources that could be properly identified with late type cluster members and had at least about 1000 source counts. The identification of the X-ray sources was taken from the literature (mainly from the prime reference given in Table 1) and checked by comparing optical and X-ray positions. Background spectra were extracted from nearby source free regions. We only used spectra of unblended sources, where no problems due to other nearby sources occurred. Furthermore, we investigated the X-ray light curves of all sources and excluded objects showing strong variability or flares. This resulted in 62 X-ray spectra for 56 different stars. The background subtraction and the rebinning of the spectra was performed with the corresponding EXSAS

Table 1. Basic information on the stellar sample and the ROSAT data sets (identified by their observation numbers ROR) used for this study.

	ROR	D [pc]	age [Myrs]	Ref.
Clusters				
Orion	200151	500	≈ 1	1
ρ Oph	200045	160	≈ 1	2
Cha I	200207	140	$\lesssim 10$	3
IC2391	200501	160	40	4
Pleiades	200557, 200068 200008, 200556	125	70	5
Hyades	200020, 200777 201368, 200443 200776, 800193 200913, 201369	45*	600	6
Field stars				
EK Dra	201474	31	70	7
π^1 UMa	200654	14	300	7
χ^1 Ori	200794	10	300	7
HD 1835	201470	20	600	7
κ^1 Cet	200796	9.4	700	7
β Com	201471	8.3	1600	7
15 Sge	201475	17	1900	7
β Hyi	200071	6.3	9000	7

*: Whenever possible, individual distances as given by Stern et al. (1995) have been used.

Code for References: 1: Gagné et al. (1995a);

2: Casanova et al. (1995); 3: Feigelson et al. (1993);

4: Patten & Simon (1993); 5: Stauffer et al. (1994);

6: Stern et al. (1995); 7: Güdel et al. (1996a,b)

routines. We used a flexible binning scheme, in which channels are added to a bin until a signal to noise ratio of $S/N \geq 5$ is reached inside this bin. This binning scheme makes optimal use of the available spectral information and avoids bins with nearly zero source counts.

3. Spectral modeling

3.1. Possible spectral models

The simplest spectral model for coronal sources is isothermal plasma emission (1T model). In this model the X-ray flux S_X the satellite receives at energy E is

$$S_X(E) = \frac{1}{4\pi D^2} e^{-\sigma(E)N_H} EM \Lambda(E, T)$$

where D is the distance to the source, N_H is the hydrogen column density along the line of sight, $\sigma(E)$ is the extinction cross section of the interstellar matter, EM is the emission measure, T the plasma temperature, and $\Lambda(E, T)$ the emissivity of the coronal plasma. This model has three parameters, N_H , EM , and T .

Table 2. Properties of the sample stars (for details see text).

star	SpT	R_* [R_\odot]	$v \sin i$ [km/s]	P_{rot} [d]	rem	star	SpT	R_* [R_\odot]	$v \sin i$ [km/s]	P_{rot} [d]	rem
Orion						Pleiades					
P1659	K1	5.1	< 20	17.25	W	H _z 1136	G8 V	0.69	75	0.52	bin?
P1784	K2 V	6.8		8		H _z 2034	K2.5 V	0.72	77	0.36	
P1955	G1 III	5.8	109			H _z 2147	K0 V	1.00	27		bin?
ρ Oph						H _z 2500	F9.5 V	1.20	30		
SR 12	M1		21		W	H _z 3197	K3 V	0.71	33		bin?
SR 9	K5-7e		16		C	Hyades					
V853 Oph	M1.5e				C	VA 288	M3e		13.5		
DoAr 21	G,K		16			VA 627	K2				
Cha I						VB 19	F5	1.24	10		
Sz 6	K2e	2.1	37	2.3	C	VB 34	F6		12		bin
CS Cha	K5e	1.7	16		C	VB 37	F4	1.6	12		
VW Cha	K2e	2.3	26		C	VB 40	F8 IV		8		bin
Ced 110	G2	3.4	75		W	VB 50	G1 V	1.1	10	7.1	bin?
Glass 1	K3/G5				bin/W	VB 57	F7 V		18		bin
Sz 30	K8	1.8			W	VB 59	F8 V		11	4.98	bin
HM Anon	G8	1.5			W	VB 64	G2 V	1.0		8.7	
CHXR 3	K3				W	VB 71	K0 III		2.4		bin
IC 2391						VB 75	F7		10		bin
HD 74009	F3 V	1.9				VB 77	G0		25		bin
CPD-52 1602	F6 V					VB 141	F0 V		160		bin
SJHM 3	K1-3e	1.3	90			VB 190	K9	0.65	14.4	3.66	bin
Pleiades						L 86	M2	0.63	15		
H _z 253	G1	1.10	37			Field stars					
H _z 314	G1	1.10	38	1.48		EK Dra	G0 V	0.92	17	2.75	
H _z 686	K7 Ve	0.64	150	0.4		π^1 UMa	G1.5 V	1.0		4.68	
H _z 727	F9 V	1.25	50	1.2		χ^1 Ori	G1 V	1.0		5.08	
H _z 738	G9 V	0.81	50		bin?	HD 1835	G2 V	1.0		7.65	
H _z 739	G0 V	1.37	13		bin?	κ^1 Cet	G5 V	1.0	8	9.2	
H _z 761	G2 V	1.05	11			β Com	G0 V	1.0		12.4	
H _z 1032	G8	0.81	37			15 Sge	G5 V	1.0	4	13.5	
H _z 1100	K3 V	0.70	< 9		bin?	β Hyi	G2 IV	1.6		45	

A simple extension of the isothermal model is the two temperature model (2T model), with individual emission measures for the two temperature components, where the X-ray flux is given by

$$S_X(E) = \frac{1}{4\pi D^2} e^{-\sigma(E)N_H} (EM_1 \Lambda(E, T_1) + EM_2 \Lambda(E, T_2))$$

In this study we prefer a model with a continuous distribution of emission measure with temperature $EM(T)$ (CED model), where we have

$$S_X(E) = \frac{1}{4\pi D^2} e^{-\sigma(E)N_H} \int EM(T) \Lambda(E, T) \frac{dT}{T}$$

and assume a power-law dependence up to a maximum temperature

$$EM(T) = \begin{cases} EM_0 \left(\frac{T}{T_{\text{max}}}\right)^\alpha & \text{for } 10^5 \text{K} \leq T \leq T_{\text{max}} \\ 0 & \text{else} \end{cases}$$

This model has four parameters, N_H , EM_0 , T_{max} , and α .

The use of more complicated spectral models seems not to be reasonable, keeping in mind the quite moderate spectral resolution of the PSPC (see also our discussion in the Appendix).

3.2. Selection of a spectral model

Before deciding which spectral model to use, we have tentatively applied all three models to our spectra and obtained the following results: successful 1T fits can be found for only a few spectra, especially those with a low number of counts and rather high extinction. The 2T model gives acceptable fits to nearly all spectra of our sample. Finally, the CED model gives acceptable fits to all spectra. For most sources, the ‘‘goodness’’ of the fit as measured by χ^2_{red} (see below), is very similar for the 2T model and the CED model. As an example of the fitting success of the three models we show in Fig. 1 the best fits for the spectrum of the Hyades stars VB 40.

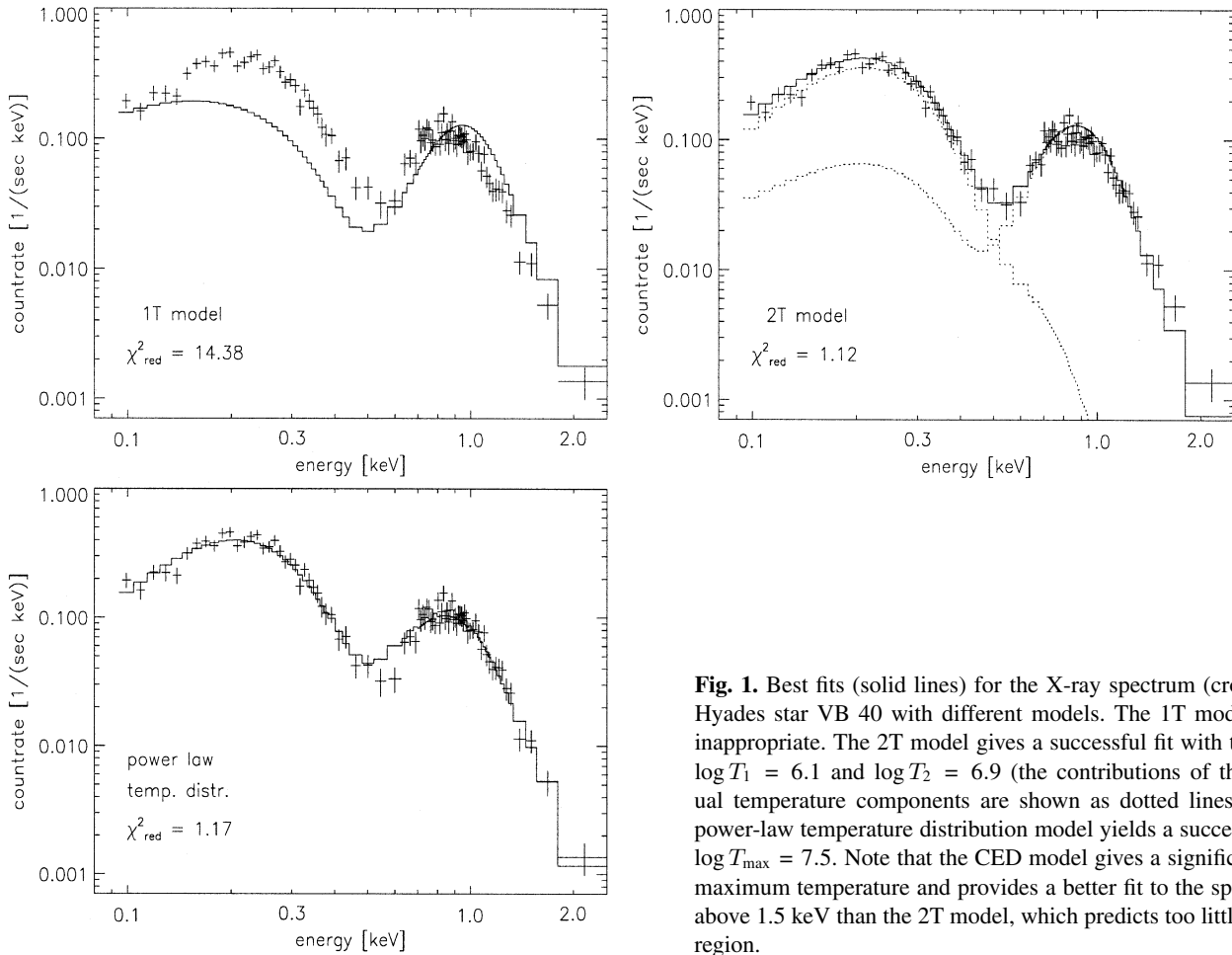


Fig. 1. Best fits (solid lines) for the X-ray spectrum (crosses) of the Hyades star VB 40 with different models. The 1T model is clearly inappropriate. The 2T model gives a successful fit with temperatures $\log T_1 = 6.1$ and $\log T_2 = 6.9$ (the contributions of these individual temperature components are shown as dotted lines). The CED power-law temperature distribution model yields a successful fit with $\log T_{\max} = 7.5$. Note that the CED model gives a significantly higher maximum temperature and provides a better fit to the spectral region above 1.5 keV than the 2T model, which predicts too little flux in this region.

These fitting results are very similar to those reported by other authors: the 1T model fails to fit nearly all high quality stellar X-ray spectra because it is obviously too simple to adequately describe stellar coronae, that can by no means be expected to be isothermal. On the other hand, most ROSAT spectra of late type stars can successfully be fitted with a 2T model (e.g. Stern et al. 1994; Gagné et al. 1995b). However, it should be noted that at least for some very high quality ROSAT spectra the 2T model seems to be no longer appropriate (Ottmann 1994). Furthermore, observations of the same sources with different instruments have revealed systematic differences in the results of 2T fits, which suggests that the temperature solutions may be partially dependent on the detector (Majer et al. 1986). It is also important to note that a successful 2T fit does not necessarily imply the presence of two physical distinct regions that correspond to the different temperatures (see Appendix).

The CED model has been used by Schmitt et al. (1990), who found that the EINSTEIN spectra of late type stars could be well fitted with this model. Nevertheless, from the fitting results alone it is not obvious whether the 2T model or the CED model is preferable, since in the absence of independent information there is no way to distinguish between two models that fit the data equally well. Furthermore, we have performed spectral fitting simulations (see Appendix) that show that the

spectral resolution of the PSPC is not high enough to permit a strict distinction between these models: simulated spectra based on a CED model can very often be successfully fitted with a 2T model. Only observations with considerably higher spectral resolution can reveal the true coronal temperature distribution and decide between both models. In this context, it is important to keep in mind that the 1T and 2T models provide only a very simple parameterization of the coronal temperature structure and can probably not be expected to yield a physically consistent description of coronae. We believe that the CED model, although it is also rather simple, might describe a corona in a more physical manner than the 2T model (see also Schmitt et al. 1990). This is based on the following arguments:

Spatially resolved observations of the solar corona show that the coronal loops exhibit a *continuous* temperature variation from chromospheric temperatures up to the maximum temperature (e.g. Vaiana & Rosner 1978; Hara et al. 1992). Theoretical loop models (see e.g. Antiochos & Noci 1986; Maggio & Peres 1996) as well as solar observations (see e.g. Dere & Mason 1993; Bruner & McWhirter 1988) yield coronal temperature distributions very similar to the power-law form used in the CED model. Typical parameters inferred from solar extreme-ultraviolet or X-ray observations are $\alpha \approx 1.5$ from $\log T \approx 5.0$ to $\log T \approx 6.4$. In nearly all solar emission measure distribu-

tions a rather pronounced minimum is found near 10^5 K (see Bruner & McWhirter 1988). This lack of material at this temperature can be explained by the maximum of the radiative loss function around $\approx 10^5$ K (see Doyle et al. 1985) and is the reason for our choice of the lower boundary of the temperature distribution at 10^5 K. Since the contribution of material at temperatures below and slightly above 10^5 K to the X-ray flux in the 0.1 – 2.4 keV ROSAT band can be fully neglected (see Raymond & Smith 1977; Raymond 1988), our choice of 10^5 K as the lower boundary of the temperature distribution is not critical with respect to the results.

There is also evidence for continuous emission measure distributions in the coronae of late type stars: for nearly all late type stars observed with EUVE, broad continuous temperature distributions are found (e.g. Schrijver et al. 1995), in many cases very similar to power-laws (e.g. Haisch et al. 1994; Drake et al. 1995). In a recent review on EUVE spectroscopy of late type stars Drake (1996) concludes that there are no 2T coronae and a continuous temperature distribution is necessary to explain the spectra.

We are aware that the CED model is also a rather simple description of the coronal temperature structure. While the true temperature distribution is most likely continuous, it will not necessarily be of a power law form since there might be different types of loops with different lengths, temperatures, and pressures. It might even be possible that in some cases (e.g. when there are two dominant families of different loops) the temperature structure is actually more similar to a 2T model than to a power law distribution. Indeed, for some stars, high resolution X-ray and EUV spectra indicate temperature distributions with rather pronounced peaks at a few dominant temperatures (e.g. for AB Dor; Mewe et al. 1996).

However, for most late type stars observed with EUVE there is no evidence for a significant bimodal temperature structure and the common morphology of the temperature distributions is rather similar to the power-law distributions of the CED model (Drake 1996). We think the CED model provides a good compromise between the physical expectations for the actual temperature distribution and the amount of information available in modest resolution X-ray spectra. The use of more complicated models (e.g. a sum of power laws with different maximum temperatures and slopes) is not meaningful, keeping in mind the rather low spectral resolution of our PSPC data.

Furthermore, the CED model has the additional advantage that the parameters T_{\max} and α have a clear physical meaning, giving simply the highest temperature present in the corona and the relative amount of hot versus cool plasma. This is not the case for the 2T model, where one has to define some “characteristic” temperature before investigating possible dependences on other stellar quantities. It is not clear, how such a quantity should be obtained from the results of a 2T fit and still have a physical meaning. Indeed, different studies use quite different definitions: e.g. Gagné et al. (1995b) use an emission measure weighted mean of the two temperatures, while Güdel et al. (1996a) consider only the high temperature component.

3.3. Fitting procedure and results

The recent version of the Raymond & Smith model of optically thin thermal plasma emission (see Raymond & Smith 1977; Raymond 1988) was used to calculate the model spectra. For the extinction cross sections we used the Morrison & McCammon (1983) model. Solar abundances were assumed for the plasma and the interstellar matter. For some stars in our sample, information on the optical extinction A_V can be found in the literature and one can calculate the hydrogen column density from the relation $N_H = A_V \times 1.8 \times 10^{21} \text{ cm}^{-2}$ (Paresce 1984; Predehl & Schmitt 1995). Nevertheless, we decided to treat N_H as a free fitting parameter, especially since, at least for TTS, the estimation of extinction is rather difficult and uncertain. If optical extinction information was available, we checked the concordance of the fitted extinction with the optical value and found rather good agreement in nearly all cases. It should be noted that a fitted extinction of $\log N_H \lesssim 19.5$ is merely significant and often is consistent with even no extinction.

In the fits N_H could take values between 10^{18} and 10^{24} cm^{-2} , T_{\max} was allowed to vary between 10^5 and $10^{8.5}$ K, and no limits were imposed on EM_0 and α . The best fit model was determined with a χ^2 fitting routine using the Levenberg-Marquardt method; the resulting quantity χ_{red}^2 is a measure for the quality of the fit (Press et al. 1986). From χ_{red}^2 one can calculate the statistical acceptance Q , which gives the probability that the deviations between the source spectrum and the model spectrum are only due to statistical measurement errors (see Press et al. 1986). We defined fits as “acceptable” if $Q > 0.01$, and could find acceptable fits for all spectra of our sample. To quantify the uncertainties of the fitting parameters we derived confidence intervals for the fitting parameters from χ^2 grids using the projection method described by Lampton et al. (1976). Since in most aspects of the following analysis we are interested only in T_{\max} , we determined 1- σ confidence intervals for the case of independent variables.

In Table 3 we summarize the results of our spectral fits. We give the number of the ROSAT data set from which the spectrum was extracted, the number of source counts per spectrum, the “best-fit” parameters together with the limits of the 1- σ confidence intervals for T_{\max} and α , and χ_{red}^2 . We have also calculated the X-ray luminosities L_X in the ROSAT band (0.1 – 2.4 keV) from the spectral parameters. A comparison of our values with the X-ray luminosities derived by other authors (see references to Tab. 1) from the same ROSAT data show generally good agreement within the errors. We are aware that maximum temperatures above 10^8 K are rather uncertain, since the PSPC is not very sensitive to such high temperatures. Nevertheless, they indicate the presence of very hot plasma.

4. Possible problems: temporal variability and abundance variations

Before we start with the interpretation of our fitting results, we briefly discuss two effects that could in principle affect our results.

Table 3. Results of the CED model fits to the X-ray spectra.

star	ROR	counts	$\log N_{\text{H}}$ [cm^{-2}]	$\log T_{\text{max}}$	min	max	α	min	max	$\log L_{\text{X}}$ [erg/sec]	χ_{red}^2
Orion											
P1659	200151	668	21.1	7.9	7.6	8.2	1.1	0.6	2.0	31.7 ± 0.3	0.78
P1784	200151	1622	21.1	8.1	8.0	8.4	1.2	0.8	1.5	32.1 ± 0.3	0.96
P1955	200151	1055	21.5	7.8	7.6	8.1	1.2	0.3	2.0	32.1 ± 0.3	1.12
ρ Oph											
SR 12	200045	2120	20.8	8.3	8.0	8.5	0.4	0.2	0.6	30.6 ± 0.2	1.15
SR 9	200045	2372	21.1	7.5	7.5	7.6	2.0	1.5	2.2	30.7 ± 0.3	0.87
V853 Oph	200045	1793	20.6	7.9	7.7	8.2	1.4	1.0	1.8	30.5 ± 0.2	0.86
DoAr 21	200045	3165	21.8	7.1	7.0	7.2	6.2	0.5	9.0	31.9 ± 0.3	1.03
Cha I											
Sz 6	200207	1079	20.6	7.3	7.3	7.4	4.6	3.8	5.4	30.3 ± 0.2	1.15
CS Cha	200207	2382	20.8	7.8	7.8	8.2	0.4	0.2	0.4	30.5 ± 0.2	0.94
VW Cha	200207	1442	21.4	7.5	7.5	7.7	1.7	1.4	2.2	30.5 ± 0.3	0.80
Ced 110	200207	1533	21.8	7.4	7.2	7.6	1.5	0.8	8.0	31.0 ± 0.4	0.60
CHX 12	200207	802	21.0	7.6	7.4	7.6	1.9	1.9	3.5	30.0 ± 0.2	1.18
Sz 30	200207	1963	21.0	7.8	7.7	8.2	0.6	0.3	0.8	30.5 ± 0.2	0.89
HM Anon	200207	1376	21.3	7.4	7.3	7.5	2.0	0.3	2.7	30.5 ± 0.3	1.00
CHXR 3	200207	850	21.7	7.9	7.4	8.1	1.4	0.1	2.3	30.6 ± 0.4	0.45
IC 2391											
HD 74009	200501	2728	19.7	7.8	7.7	8.0	0.7	0.6	0.9	30.7 ± 0.2	1.32
CPD -52 1602	200501	1141	20.3	7.5	7.3	7.7	0.2	0.0	0.4	30.3 ± 0.2	1.56
SJHM 3	200501	967	19.7	8.4	8.0	8.5	0.6	0.5	1.0	30.2 ± 0.2	0.80
Pleiades											
Hz 253	200557	2950	20.5	7.5	7.5	7.7	1.3	1.1	1.5	30.5 ± 0.2	1.04
Hz 314	200557	2221	20.3	7.8	7.7	8.0	0.5	0.3	0.8	30.3 ± 0.2	1.04
Hz 686	200557	656	20.4	7.7	7.2	8.1	0.0	0.0	0.3	30.0 ± 0.2	0.81
Hz 727	200008	1146	20.2	7.3	7.1	7.5	0.9	0.3	1.8	29.8 ± 0.2	0.88
Hz 738	200068	1116	20.8	7.3	7.2	7.4	3.1	3.1	4.1	30.0 ± 0.2	0.91
Hz 739	200557	1399	20.0	7.3	7.2	7.4	1.5	1.3	1.8	30.0 ± 0.2	0.70
Hz 761	200068	1007	20.2	7.2	7.0	7.4	0.4	0.0	1.0	29.8 ± 0.2	1.11
Hz 761	200008	923	20.0	7.3	7.1	7.5	0.6	0.3	1.1	29.6 ± 0.2	1.00
Hz 1032	200068	1676	20.6	8.0	7.7	8.5	0.7	0.3	1.0	30.2 ± 0.2	1.02
Hz 1032	200008	1878	20.6	8.0	7.7	8.4	0.5	0.2	0.8	30.1 ± 0.2	0.96
Hz 1100	200068	740	20.5	8.0	7.6	8.5	0.5	0.1	1.0	29.8 ± 0.2	0.83
Hz 1136	200068	1289	20.7	8.2	7.8	8.5	0.5	0.3	0.8	30.1 ± 0.2	0.94
Hz 2034	200068	549	20.1	7.4	7.2	7.5	1.8	1.1	3.9	29.5 ± 0.2	0.93
Hz 2147	200068	4061	20.2	7.7	7.6	7.9	0.8	0.6	0.9	30.5 ± 0.2	1.06
Hz 2147	200556	2309	20.1	7.8	7.8	8.1	1.1	0.8	1.2	30.5 ± 0.2	1.05
Hz 2500	200008	2479	20.3	7.8	7.5	8.5	0.3	0.1	0.7	30.3 ± 0.2	1.47
Hz 2500	200556	1837	20.3	7.7	7.5	7.8	0.5	0.3	0.8	30.4 ± 0.2	0.97
Hz 3197	200556	1035	20.2	7.8	7.5	8.1	0.7	0.4	1.1	30.1 ± 0.2	0.79

The first are X-ray flares, which are known to cause temporary variations in the spectral parameters (e.g. Ottmann & Schmitt 1994; Pan & Jordan 1995). Since we excluded all flaring or strongly variable sources from this study, our data should not be affected by, at least strong flares. However, there still might be variability on amplitudes below the noise level of the light curves. We can investigate temporal variability in the spectral parameters of four Pleiades stars and two Hyades stars, for which we have spectra from two different ROSAT observations. For none of these stars (Hz 761, Hz 1032, Hz 2147, Hz 2500,

VB 71, and VB 141) significant variations of the spectral parameters can be found. Thus, we conclude that spectral variability is not expected to affect the results of our study.

Another problem might be caused by deviations in the elemental abundances of the coronal plasma from the assumed solar abundances. Recent results, especially from ASCA and EUVE observations, have revealed an under-abundance of metals relative to photospheric values by factors between 2 and 10 in the coronae of some, but not all, late type stars (e.g. Drake et al. 1996ab; Singh et al. 1996). Furthermore, some late type stars

Table 3. (continued)

star	ROR	counts	$\log N_{\text{H}}$ [cm^{-2}]	$\log T_{\text{max}}$	min	max	α	min	max	$\log L_{\text{X}}$ [erg/sec]	χ_{red}^2
				[K]							
Hyades											
VA 288	200020	3692	19.5	8.0	7.8	8.2	0.1	0.0	0.1	29.1 ± 0.2	1.31
VA 627	200443	952	19.3	7.8	7.5	8.2	0.0	0.0	0.1	28.8 ± 0.2	1.40
VB 19	800193	2693	19.8	7.2	7.1	7.4	0.0	0.0	0.1	29.5 ± 0.2	1.45
VB 34	200776	2506	18.8	6.8	6.8	7.0	0.3	0.1	0.3	29.2 ± 0.2	1.19
VB 37	200776	2088	19.6	6.9	6.9	7.0	0.3	0.2	0.6	29.4 ± 0.2	1.34
VB 40	200020	5079	19.6	7.5	7.4	7.7	0.1	0.1	0.2	29.4 ± 0.2	1.17
VB 50	200020	11950	19.6	8.0	7.8	8.0	0.1	0.1	0.2	29.8 ± 0.2	1.27
VB 57	200777	3772	19.6	7.1	7.0	7.2	0.2	0.1	0.4	29.7 ± 0.2	0.82
VB 59	200777	2513	19.6	7.5	7.4	7.8	0.1	0.0	0.3	29.6 ± 0.2	0.92
VB 64	201369	1303	19.7	7.2	7.1	7.4	0.0	0.0	0.1	29.2 ± 0.2	1.13
VB 71	200777	8305	19.6	7.2	7.1	7.3	0.6	0.4	0.7	30.3 ± 0.2	1.11
VB 71	201368	8878	19.6	7.2	7.1	7.4	0.5	0.4	0.6	30.4 ± 0.2	1.11
VB 75	201368	1470	19.6	7.6	7.3	8.1	0.1	0.0	0.2	29.5 ± 0.2	0.99
VB 77	200443	2203	19.8	7.2	7.0	7.6	0.0	0.0	0.4	29.6 ± 0.2	0.90
VB 141	200020	20308	19.4	7.8	7.7	8.0	0.3	0.2	0.3	30.2 ± 0.2	1.06
VB 141	200777	11237	19.2	7.8	7.7	8.0	0.4	0.2	0.5	30.2 ± 0.2	1.06
VB 190	201368	1256	19.4	8.4	8.3	8.5	0.5	0.4	0.7	29.7 ± 0.2	1.64
L 86	200913	1156	19.6	8.4	8.0	8.5	0.1	0.0	0.2	29.1 ± 0.2	1.51
Field stars											
EK Dra	201474	4375	19.6	7.5	7.4	7.5	0.3	0.2	0.4	29.9 ± 0.2	0.90
π^1 UMa	200654	30293	19.5	7.2	7.1	7.2	0.1	0.0	0.3	29.2 ± 0.1	0.94
χ^1 Ori	200794	2342	18.7	7.2	7.2	7.3	0.2	0.0	0.3	29.1 ± 0.1	1.32
HD 1835	201470	2333	19.0	7.2	7.0	7.3	0.3	0.2	0.5	29.1 ± 0.2	1.20
κ^1 Cet	200796	700	18.7	7.3	7.2	7.4	0.1	0.0	0.2	28.9 ± 0.2	1.02
β Com	201471	3158	18.7	6.7	6.5	6.8	0.1	0.0	0.3	28.2 ± 0.2	0.93
15 Sge	201475	436	18.0	6.8	6.7	6.8	0.0	0.0	0.1	28.1 ± 0.2	1.11
β Hyi	200071	133	19.0	6.3	6.0	6.5	1.5	0.5	2.5	27.0 ± 0.2	0.64

seem to exhibit some kind of FIP-effect¹ (cf. Drake et al. 1996a), while others do not (cf. Drake et al. 1995) and still others show abundance variations with strong deviations from the usual FIP-effect (cf. Drake et al. 1994). On top of that, it should be noted that even the solar FIP-effect is neither fully understood (e.g. Henoux 1995) nor without controversy (cf. Phillips et al. 1995).

Since the abundance variations are far from being well established, the limited spectral resolution of the PSPC actually prevents the derivation of good constraints on elemental abundances, and for nearly all stars in our sample no information about possible abundance variations is available, we have assumed solar abundances for fitting the X-ray spectra. To investigate the possible impact of assuming wrong abundances we have performed spectral fitting simulations (see Appendix). Our simulations show that the assumption of wrong abundances is not expected to cause serious errors in the derived coronal temperatures. Over- or underestimations of the temperatures up to a factor of two might occur, what merely exceeds the uncertainties in our fitted maximum temperatures.

¹ In the solar corona elements with a low first ionization potential are over-abundant relative to those with a high first ionization potential by factors up to 10 with respect to the photosphere (e.g. Meyer 1985).

5. Results

5.1. Spectral parameters

In Fig. 2 we plot the fitted parameters T_{max} and α for all stars of our sample. We have also included the Sun, assuming typical values of $\log L_{\text{X},\odot} = 27.3$, $\log T_{\text{max},\odot} = 6.4$, and $\alpha = 1.5$. With the exception of the “old sun proxy” β Hyi, all stars show significantly higher maximum temperatures than the Sun. On the other hand, no obvious difference is found in the spectral parameters for stars of different age. The TTS show spectral parameters similar to those of some much older stars in the Pleiades and Hyades. All TTS show $\alpha \gtrsim 0.3$, indicating a relatively high fraction of hot plasma.

It should be noted that the values for T_{max} found in our fits in many cases considerably exceed the high temperature component from 2T fits for the same spectra (e.g. see Fig. 1). We interpret this as a hint that there is in fact a continuous temperature distribution and the 2T model underestimates the maximal temperature. Strong evidence for this assumption is found in the cases of EK Dra and κ^1 Cet, where ASCA spectra are also available (see Güdel et al. 1996a): for EK Dra we find $\log T_{\text{max}} = 7.5$, while the 2T fit to the ROSAT spectrum gives a considerably

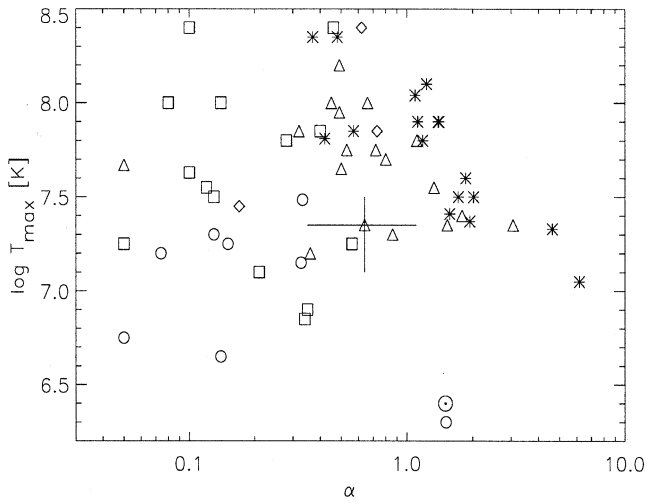


Fig. 2. Spectral parameters of all stars of our sample. For the TTS (Orion, ρ Oph, and Cha I) we use asterisks, diamonds for the stars in IC2391, triangles for the Pleiades, squares for the Hyades, and circles for the solar type field stars. The Sun is marked with \odot . Here and in most of the following plots error bars are omitted for clarity. To indicate the typical size of the uncertainties we show error bars for one Pleiades star.

cooler high temperature component of $\log T_2 = 7.0$. However, the fit to the ASCA spectrum requires a strong third temperature component at $\log T_3 = 7.4$ (Güdel et al. 1996a), which clearly demonstrates the presence of significantly hotter plasma than found in the 2T ROSAT fit and is fully consistent with our maximum temperature. Furthermore, we can even explain the difference between T_2 and T_{\max} : in our spectra fitting simulations (see Appendix), we show that the most probable value to be found in a 2T fit to a CED spectrum with $\log T_{\max} = 7.5$ is $\log T_2 \approx 7.1$, fully consistent with our fitting result for EK Dra. Qualitatively similar results are found for κ^1 Cet.

In the following analysis we will investigate the relation of the spectral parameters to basic stellar properties. Therefore we exclude all known or suspected binaries from our sample, since one cannot know from which star in an unresolved binary system the X-rays originate.

5.2. Coronal temperature and spectral type

The first aspect to investigate is the dependence of the coronal temperature on the spectral type. In several studies it has been found that K and M stars show higher coronal temperatures compared to F and G stars (e.g. Schmitt et al. 1990; Stern et al. 1994). We cannot confirm this trend and find no significant dependence of the temperatures on the spectral type in our sample. Only if we focus on the Hyades stars a correlation seems to be present. However, no such correlation exists for the Pleiades stars (see Fig. 3) or for the other stars. This can be explained by the rotational velocities of these stars, as will be shown later. In any way, the spectral type seems not to determine the coronal temperatures.

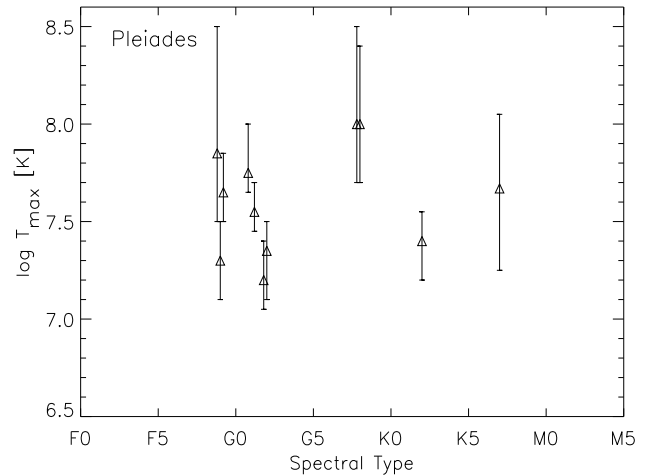
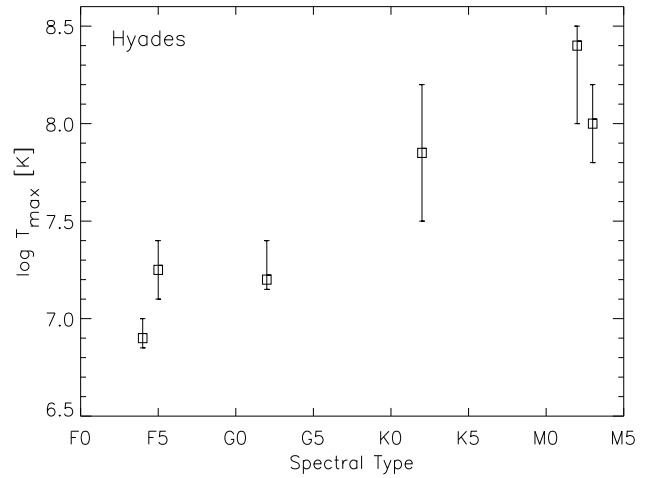


Fig. 3. The dependence of the maximum temperatures on the spectral type for the Hyades and Pleiades stars in our sample.

We have also investigated possible relations of the coronal temperatures to the stellar mass, radius and surface gravity, but could not find any correlation.

5.3. Amplitude of X-ray emission and stellar rotation

It is well known that the X-ray luminosity of late type stars scales with rotation (Pallavicini et al. 1981). This is generally interpreted as a link between the coronal heating and the production of magnetic flux by a solar type dynamo. In Fig. 4 we plot the X-ray luminosity L_X against the rotational velocity and the X-ray surface flux F_X against the rotational period. The stars in our sample show the same dependencies as found in other studies: For slowly rotating stars the amplitude of the X-ray emission increases with rotation, whereas for fast rotators a saturation effect occurs. Very similar relations have been found for main-sequence stars (e.g. Dorren et al. 1995; Stauffer et al. 1994) as well as for TTS (e.g. Bouvier 1990; Gauvin & Strom 1992). This indicates that the amplitude of the X-ray emission is mainly determined by the rotation and related to the stellar age by the rotational evolution of the young stars (cf. Bouvier 1994 and

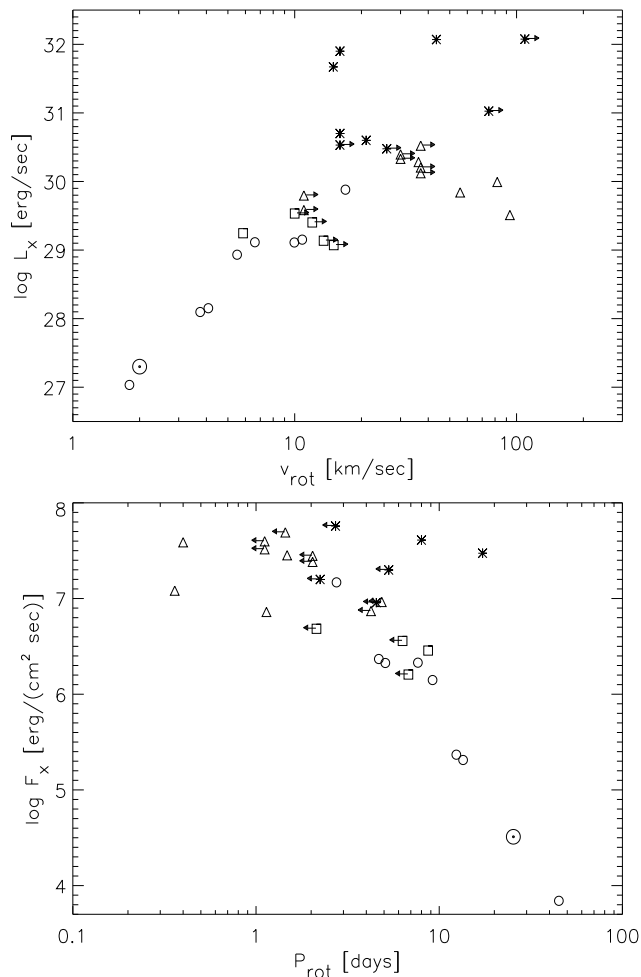


Fig. 4. The dependence of the X-ray emission on the stellar rotation. Symbols with arrows denote objects with unknown rotational period for which lower limits to the rotational velocity resp. upper limits to the rotational period have been calculated from $v \sin i$. The number of data points in the lower plot is somewhat smaller due to unknown radii for some stars. The meaning of the symbols is as in Fig. 2

Stauffer 1994). Only the Orion TTS P1659 and P1784 show a significantly higher X-ray surface flux than to be expected from their rotational periods, what might perhaps be explained by differential rotation (see Smith 1994).

5.4. Coronal temperature and X-ray activity

Further information can be gained by looking for a relation between the coronal temperature and the amplitude of the X-ray emission. Our data show a clear correlation between T_{\max} and L_X , although the scatter is rather large (upper plot in Fig. 5). Similar correlations between the coronal temperature and the X-ray luminosity have already been reported in other studies. For example, Schmitt et al. (1990) found a correlation $L_X \propto T^{2.5}$ from 1T fits to the EINSTEIN spectra of late type stars and Güdel et al. (1996a,b) found $L_X \propto T_2^4$ from 2T fits to the ROSAT

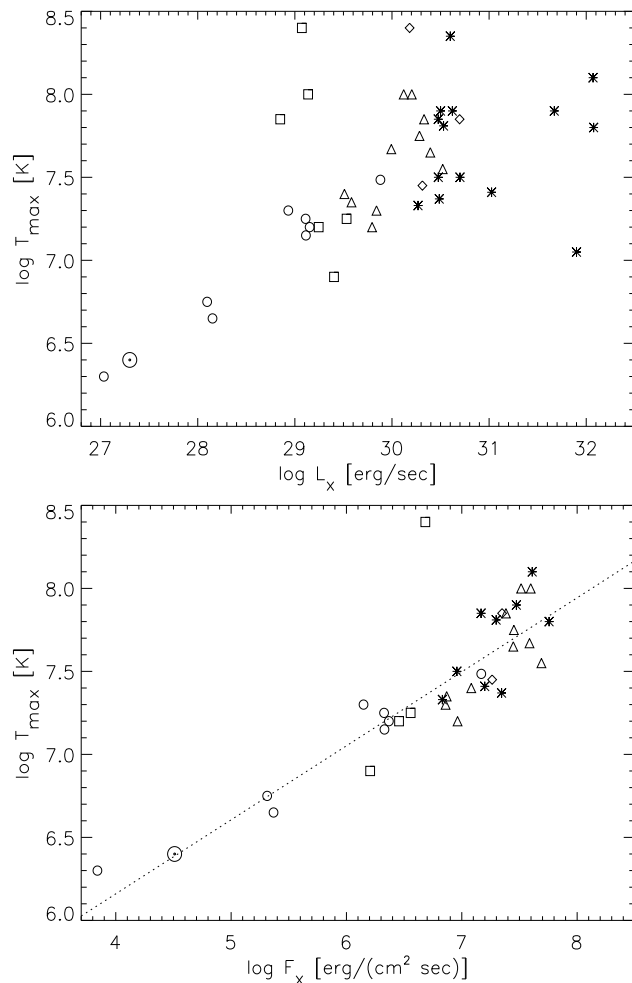


Fig. 5. Maximum temperature versus X-ray luminosity (upper plot) resp. surface X-ray flux (lower plot). The dotted line indicates the best fit found in the linear regression analysis for F_X and T_{\max} . The meaning of the symbols is as in Fig. 2.

spectra of their sample of solar type field stars also used in our study.

If we use F_X instead of L_X (lower plot in Fig. 5), we find a much better correlation, extending over nearly two orders of magnitude in T_{\max} and four orders of magnitude in F_X . TTS, young main sequence stars and field stars follow the same relation between F_X and T_{\max} . Only the Hyades member L 86 clearly deviates from the correlation. This is a G2 star and its location in the plot might be explained by the possibility that a significant part of the X-rays originates from an (up to now unknown) late type companion. In that case, we would underestimate the surface flux considerably.

We have performed a linear regression analysis (excluding L 86) and found the best fit relation

$$\log F_X = (-9.3 \pm 0.1) + (2.2 \pm 0.2) \log T_{\max}$$

shown as the dotted line in Fig. 5. As noted by Basri (1987), the X-ray surface flux is a very good measure of stellar activity.

This explains, why the correlation between T_{\max} and F_X is much better than between T_{\max} and L_X and shows that the coronal temperatures are determined by stellar activity.

Now we are in a position to explain why the Hyades seem to exhibit a correlation between T_{\max} and the spectral type, while the other stars in our sample do not (see section 5.2). The Hyades stars in our sample have very similar rotational velocities, ranging only from 10 km/sec to 15 km/sec. Since the rotational velocity scales with the stellar radius, the later type stars have shorter rotational periods than the earlier type stars. Finally, the dependence of activity on the rotational period and that of the coronal temperature on activity explains the apparent correlation between temperature and spectral type. No such apparent correlation is found for the Pleiades stars in our sample, because they exhibit widely different rotational velocities.

So we conclude that the coronal properties of young stars and even the TTS are determined by stellar rotation. The high X-ray luminosities and coronal temperatures can be explained by the fast rotation of the young stars. The rotational slow down during the early phases of stellar main sequence evolution is accompanied by a continuous decrease of X-ray activity and coronal temperature (for a recent review on the rotational evolution of TTS and young stars we refer to Bouvier (1994) and Stauffer (1994)).

6. Interpretation in the frame of a simple analytic loop model

In this chapter we will use the loop model of Rosner et al. (1978; RTV model in the following) to interpret our results. In this model, scaling laws between the temperature at the loop top T_{\max} [K], the pressure p [dyn/cm²] at the loop base, the loop semi-length l [cm] and the energy input rate per unit volume ε [erg/(cm³ sec)] can be derived:

$$T_{\max} \approx 1.4 \times 10^3 (pl)^{1/3} \quad (1)$$

$$\varepsilon \approx 9.8 \times 10^4 p^{7/6} l^{-5/6} \quad (2)$$

By combining these scaling laws the relation

$$T_{\max} \approx 52 \varepsilon^{2/7} l^{4/7} \quad (3)$$

can be found.

According to relation (3), higher temperatures can be obtained by increasing the heating rate or the loop length, or a combination of both. For a further investigation we can derive theoretical relations between F_X and T_{\max} and compare them to our data. We assume the stellar corona to consist of identical loops with constant cross section A . In steady state, each loop radiates the same amount of energy as deposited into it due to the heating: $\varepsilon 2lA$. If N loops are present, the surface “filling factor” $f = 2NA/(4\pi R_*^2)$ gives the fraction of the stellar surface covered by loops. From this we find the surface flux to be $F_X = f \varepsilon l$. Using the scaling laws (1) and (3) we finally get:

$$F_X \approx 10^{-3} f \varepsilon^{1/2} T_{\max}^{7/4} \quad (4)$$

In a very similar way, we can derive the relation

$$F_X \approx 10^{-6} \frac{f}{l} T_{\max}^{7/2} \quad (5)$$

If we assume only the loop length to increase while the heating rate and the filling factor are kept constant, we would expect $F_X \propto T_{\max}^{1.75}$ according to (4). If, on the other hand, we assume only the heating rate to increase while the loop length and the filling factor stay constant, we would expect $F_X \propto T_{\max}^{3.5}$ according to (5). Both relations are inconsistent with the relation $F_X \propto T_{\max}^{(2.2 \pm 0.2)}$ found in our data. This means that the high temperatures are probably achieved by a combination of increased heating rate *and* larger loops.

It is important to note that the RTV model imposes a limit to the loop length: since it assumes a spatially uniform gas pressure, the loop length must not exceed the local pressure scale height, which for a fully ionized coronal plasma is given by

$$s_p [\text{cm}] \approx 5 \times 10^3 \frac{T_{\max} [\text{K}]}{g_*/g_\odot} \quad (6)$$

(see Serio et al. 1981). The scaling laws may be extended to loops longer than the pressure scale height (Serio et al. 1981), but we will not take this into account for two reasons. First, this extension introduces a multiplicative term containing the pressure scale height and thus the scaling laws can no longer be solved for T_{\max} and ε . Second, for the high coronal temperatures found for most star of our sample, the pressure scale height is already very large. For example, a star of solar mass and radius with $\log T_{\max} = 7.5$ has $s_p = 1.6 \times 10^{11}$ cm = $2.3 R_\odot$. Loops longer than this would exceed several stellar radii and it seems hardly imaginable that such long loops could be stable.

In the following analysis we assume the RTV scaling laws to be valid and the loop length to be smaller than the pressure scale height. Then, we can use this upper limit to the loop length to calculate the minimal pressure necessary to reach the observed maximum temperature according to scaling law (1). Furthermore, since we additionally know the surface X-ray flux, we can also calculate an upper limit to the surface filling factor from relation (5). The stellar masses necessary for calculating g_* were taken from Feigelson et al. (1993) for the TTS in Cha I and estimated from the spectral type for the young main sequence stars in IC2391, the Pleiades, Hyades, and the field stars. We did not try to estimate masses for the other T Tauri stars in our sample.

The results are shown in Fig. 6. In order to allow a comparison with solar values, we note that the total X-ray emission of the solar corona is dominated by active region loops with typical lengths of about 10^{10} cm (Pallavicini et al. 1981), for which our analysis gives $p_\odot \approx 0.6$ dyn/cm² and $f_\odot \approx 1.3\%$. To be more general, we take into account that the solar corona exhibits a variety of loops with rather different lengths. However, pressures found for quiescent solar loops range only from $p \approx 0.2$ dyn/cm² for extended interconnecting loops to $p \approx 5$ dyn/cm² for compact active region loops (Pallavicini et al. 1981; Yoshida & Tsuneta 1996).

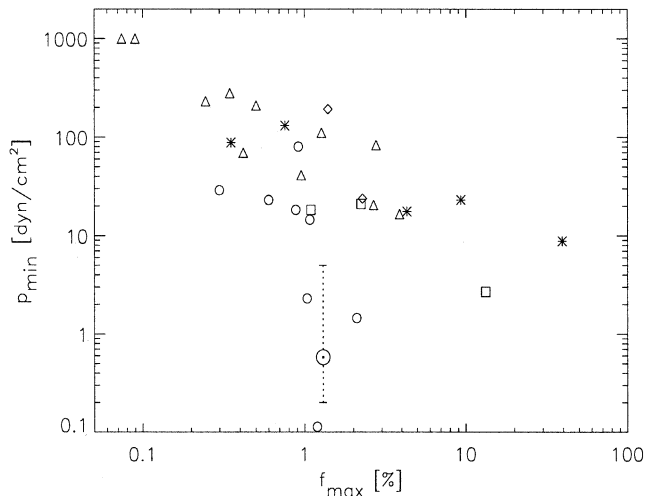


Fig. 6. The minimal pressure and the maximal filling factor calculated under the assumption that the RTV model is valid and the loop length does not exceed the pressure scale height. The error bar shows the typical range of pressures found for quiescent solar coronal loops.

The loop pressures found for most of the young stars seem to exceed typical solar values by about one or two orders of magnitude. In principle, the actual pressures could even be higher, since the actual loop length might be smaller than s_p . However, it should be noted that the typical length of solar active region loops is very similar to the pressure scale height (for $\log T_{\max, \odot} = 6.4$ formula (6) gives $s_{p, \odot} \approx 1.2 \times 10^{10}$ cm). Therefore, it seems not too unrealistic to assume $l \approx s_p$ and we believe that our results reproduce the correct order of magnitude for p and f . This means that the dominant X-ray emitting regions in the coronae of most young stars are high pressure regions that cover only a small fraction (no more than a few percent) of the stellar surface.

Of course, the validity of the rather simple RTV model may be questioned. Furthermore, these results are based on the assumption that the stellar corona is composed of loops that are all (nearly) equal. However, our findings are consistent with other recent results. In the analysis of density sensitive high-temperature emission lines in the EUVE spectra of active late type stars electron densities considerably higher than typical for solar active regions have been found (see e.g. Schrijver et al. 1995; Drake 1996).

We note that such high pressure loops require quite strong magnetic fields to confine the plasma in the loops. However, the required magnetic field strength scales only with the square root of the pressure. Since the (magnetic) activity of the young stars exceeds the solar level by far, their coronal magnetic fields might also be stronger. In this context, it seems worth noting that strong (photospheric) magnetic fields have been found on active late type stars (e.g. Valenti et al. 1995) as well as on TTS (Basri et al. 1992; Günther 1996). Furthermore, recent results provide some evidence that the strength of the magnetic surface fields may grow with stellar activity (Johns-Krull & Valenti 1996).

An alternative explanation might be suggested by the fact that the high loop pressures found for the young stars are quite similar to pressures in solar flaring loops. Although we have not included stars showing obvious flares during the ROSAT observation into our sample and could not find indications for temporal variability of the spectral parameters, we cannot exclude that the X-ray emission is nevertheless dominated by frequent low-amplitude flares, so-called “microflares”. Based on theoretical (e.g. Parker 1988) as well as observational (e.g. Porter et al. 1987) arguments, it is suspected that microflares may be occurring permanently in the solar corona and might be of importance for the coronal heating (Watanabe 1996, Yoshida & Tsuneta 1996). There are also some observational results that might indicate microflaring activity in the coronae of other active stars (e.g. Robinson et al. 1995), but a convincing proof of stellar microflares is still missing (for a recent discussion see Haisch & Schmitt 1996). Thus microflaring is a possible but not yet conclusive interpretation of these results.

7. Conclusions and summary

In our study of the coronal properties of young stars we show that the X-ray spectra can be well fitted with a continuous emission measure distribution assuming a power-law temperature dependence. We argue that this model might describe the coronal plasma in a more physical way than the frequently used 2T model. Although the fitting results alone do not allow to decide which model better describes the coronal temperature structure, our assessment is supported by recent extreme ultraviolet and X-ray observations with higher spectral resolution. In spectral fitting simulations we show that a fit with a 2T model can significantly underestimate the maximum coronal temperature if there is a continuous temperature distribution in the emitting plasma. We also show that possible abundance variations are not expected to strongly adulterate the plasma temperatures inferred from spectral fits to PSPC spectra, compared to the intrinsic uncertainties of the fitted temperatures.

While we can find no correlation between the coronal temperature and basic stellar parameters such as spectral type, mass, radius or surface gravity, a clear dependence on the X-ray activity is found. Our data show a very good correlation according to $F_X \propto T_{\max}^{(2.2 \pm 0.2)}$, extending over several orders of magnitude. This means that the high level of magnetic activity found for many young stars is determined not simply by a larger filling factor but also by the presence of higher temperature plasma. Since the very young TTS as well as the much older main-sequence stars in our sample follow the same relation, we conclude that the coronal temperatures are not directly related to stellar age. In accordance to other studies we find the X-ray activity to be determined by stellar rotation. This means that the high coronal temperatures of young stars are ultimately caused by their fast rotation.

Assuming that the coronae are composed by equal X-ray emitting loops that are consistently described by the RTV loop model and have lengths not exceeding the pressure scale height, we find that the dominant X-ray emitting structures in the coro-

nae of the young stars must be high-pressure loops that cover only a rather small fraction of the stellar surface. Such loops are quite different from solar active region loops and might be related to the very strong magnetic activity of the young stars. Alternatively, the high pressures might also be taken as an indication of microflaring activity.

Although our results depend on the validity of our, necessarily quite simplifying, model assumptions, they are in good agreement with recent results of high resolution EUV and X-ray spectroscopy. Nevertheless, it is worth checking how strongly the results depend on the use of the CED model. If one would assume a 2T model to be actually more realistic and use T_2 instead of T_{\max} , the basic results would change only slightly: One would also find a relation between F_X and T_2 , however with a decreasing slope for $\log T > 7.0$. In the loop model analysis one would find pressures up to one order of magnitude lower for the objects with the highest temperatures. However, these pressures would still be significantly higher than in typical solar active region loops. Our basic conclusion would thus remain unchanged.

Acknowledgements. I want to thank Jürgen Schmitt for helpful discussions and the referee for his comments, which helped to improve this paper. This work was supported by DARA under grant 05 OR 9103 0. The ROSAT project was supported by the Bundesministerium für Bildung, Wissenschaft, Forschung und Technologie (BMBF/DARA) and the Max-Planck-Society. This research has made use of NASA's Astrophysics Data System and the SIMBAD data base.

Appendix A: spectral fitting simulations

We have performed a large number of spectral fitting simulations in order to investigate the ability of the PSPC to constrain the correct model parameters in the different spectral models, its ability to discern between different spectral models, and the influence of the instrumental sensitivity on the fitting results. The simulations were performed in the following way. First we chose spectral parameters and calculated a model spectrum with a given number of counts, which then was rebinned in the same way as a real spectrum (see section 2). To simulate an observed spectrum, in which the number of counts per bin obeys a Poisson distribution, we replaced the number N of counts in each bin by a random number drawn from a Poisson distribution with mean N . In this way we produced a set of 250 different simulated spectra per model spectrum. Then, each of these spectra was fitted and for the analysis of the resulting fitting parameters we only used the successful fits defined by a statistical acceptance $Q(\chi^2, \nu) \geq 0.01$ (see section 3.3).

Recently, similar investigations treating 1T and 2T model spectra have been published by Maggio et al. (1995). Since our results are consistent with theirs, we will focus on our simulations with CED spectra and just briefly summarize the main results of the simulations with 1T and 2T models. The temperature of an isothermal plasma can be reproduced quite well (scatter $\lesssim 15\%$ for temperatures between $\log T = 6.0$ and $\log T = 7.7$) from spectra with about 1000 counts even in the presence of considerable extinction ($A_V \lesssim 1$). The scatter in the

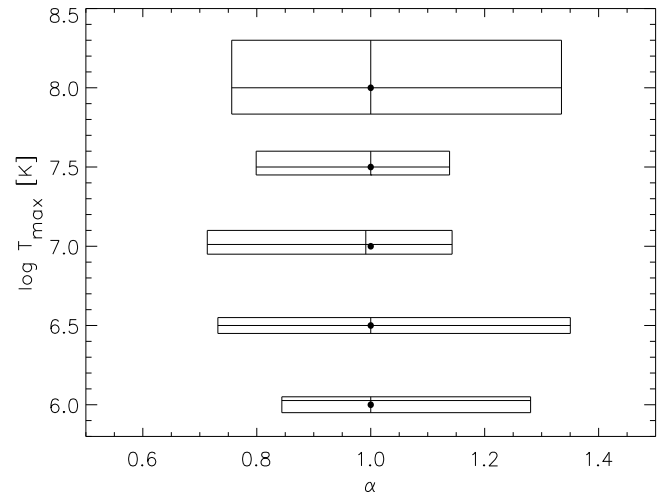


Fig. 7. Boxplot showing the results of the fits to CED spectra with different values of $\log T_{\max}$ (see text for explanation).

fitted temperatures is lowest for $\log T \approx 6.2$ and $\log T \approx 7.0$ and grows fast for $\log T \gtrsim 7.7$. This can be explained by the strongly temperature dependent sensitivity of the PSPC, caused by the peaks in the effective area for energies of 0.3 keV and 1.2 keV (see Pfeffermann et al. 1987). The temperature components of a 2T spectrum with at least 1000 counts are reproduced similarly well as long as their amplitudes are not too different ($1/5 < EM_1/EM_2 < 5/1$) and the temperatures are well separated ($\Delta T/T \gtrsim 0.15$).

A.1. Simulations with CED models

In a first set of simulations we investigated how well the spectral parameters of the CED model are reproduced. As an example we show in Fig. 7 the distributions of the fitting parameters for simulated CED spectra with $\log N_H = 20$, $\alpha = 1$, about 1000 counts per spectrum and five different values of $\log T_{\max}$ (6.0, 6.5, 7.0, 7.5, 8.0). The boxes show the intervals containing 63% of the fitting results (“1 σ -intervals”) for $\log T_{\max}$ and α . The median of the fitted values for $\log T_{\max}$ and α lie at the crossing of the lines within the boxes; the solid dots show the true spectral parameters. The number of successful fits was typically about 240 per set of 250 simulated spectra.

We also performed simulations for other values of N_H and α . Since the results are qualitatively similar we do not present them here. The results of these simulations can be summarized as follows: the 1- σ interval of the fitted maximum temperature is within $\approx 10\% - 20\%$ of the true values for models with $\log T_{\max} \leq 7.0$. For very high maximum temperatures ($\log T_{\max} > 7.7$) the scatter is up to 50%. This means that the maximum temperature can be reproduced equally as well as the temperature of an isothermal plasma spectrum. The 1- σ intervals for α are typically $\approx 30\%$. This proves that the results of the fits with CED models are meaningful.

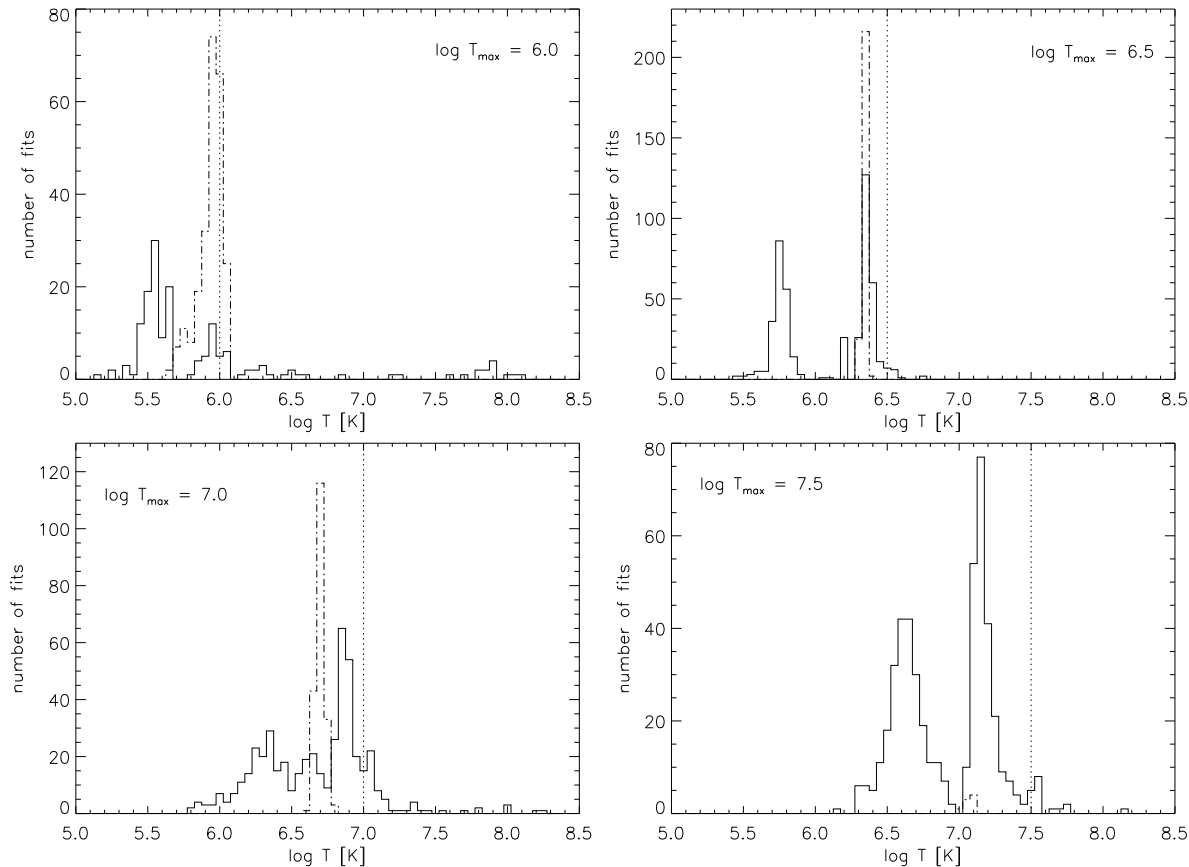


Fig. 8. Histograms showing the temperatures found in successful 1T (dashed-dotted line) and 2T (solid line) fits to sets of 250 simulated CED spectra with $\alpha = 1$, $\log N_{\text{H}} = 20$, 1000 counts per spectrum and different maximum temperatures.

A.2. 1T- and 2T-fits to CED spectra

In many studies coronal X-ray spectra are fitted with 1T or 2T models, whereas the true temperature distribution might be continuous. Thus it is very interesting to investigate the results of spectral fits with 1T and 2T models to spectra with a continuous temperature distribution.

First of all, we want to investigate whether one can prove the existence of a continuous temperature distribution from the observed spectra. This was done by simulating CED spectra and fitting them with 1T and 2T models. For example, we have simulated CED spectra with $\log T_{\text{max}} = 7.5$ and $\alpha = 0$ resp. $\alpha = 1$ with 200 resp. 1000 counts and different values of N_{H} . For each of these spectral models, the set of 250 simulated spectra was fitted with a 1T model, the spectra with 1000 counts also with a 2T model. In Table 4 we give the number of successful 1T or 2T fits. One can see that 1T models give successful fits only to low S/N CED spectra with rather high extinction. A 2T model, however, is very often successful in fitting the CED spectra even if the extinction is low. Only CED spectra with $\alpha < 1$ and $\log N_{\text{H}} \lesssim 19$ can usually *not* be fitted with a 2T model. This means that the PSPC is not able to properly discern between a 2T model and a CED model, given an observed spectrum with about 1000 counts. A successful fit with a 2T model does *not* prove that

Table 4. Number of successful 1T or 2T fits to sets of 250 simulated CED spectra with $\log T_{\text{max}} = 7.5$.

model	counts	$\log N_{\text{H}} [\text{cm}^{-2}]$					
		$\alpha = 0$			$\alpha = 1$		
		21	20	19	21	20	19
1T	200	238	41	5	234	186	98
1T	1000	56	2	0	67	8	0
2T	1000	241	226	134	233	243	232

there really are two dominant temperature components in the emitting plasma; the real emission measure distribution might be quite different from a 2T plasma. However, it is also clear that a successful fit with the CED model does not prove that there really is a power law temperature distribution.

Another very interesting aspect concerns the temperatures found in these fits, in which the “wrong” 1T or 2T models are used to fit simulated CED spectra. Some examples for the distribution of the fitted temperatures are shown as histograms in Fig. 8. Simulations for other values of α and N_{H} yielded qualitatively similar results. One can see that in nearly all cases the fitted temperatures do not exceed the true maximum temperature.

This means that the 1T or 2T fits usually do not yield temperatures that are not present in the actual temperature distribution. As long as $\log T_{\max} \leq 7.0$, the high temperature components found in the 2T fits are very close to the maximum temperatures. However, if $\log T_{\max} \gtrsim 7.5$, most of the temperatures found in the 1T and 2T fits are considerably lower than the maximum temperature. This can be explained by the decreasing sensitivity of the PSPC to plasma with temperatures $\log T \gtrsim 7.0$. This is a critical point in the determination of coronal temperatures: the temperatures found in 1T and 2T fits tend to “stay” around 10^7 K even if the actual maximum temperature increases to considerably higher values. This means that 1T and 2T fits can underestimate the maximum coronal temperature significantly when there is a continuous distribution of temperatures.

A.3. The influence of abundance variations on the inferred temperatures

As mentioned in section 4, indications of an under-abundance of heavier elements as compared to solar abundances have been found for the coronae of some late type stars. The rather moderate spectral resolution of the PSPC does not allow to derive good constraints on the abundances. However, a wrong assumption on abundances will adulterate the fitted temperatures. For our fits, we have assumed solar abundances, and it is interesting to investigate how strongly abundance variations could affect our fitting results.

We have calculated sets of simulated isothermal spectra with metal (all elements heavier than helium) abundances set to half ($Z = 0.5$) and 1/10 ($Z = 0.1$) of the solar value, assuming $\log N_{\text{H}} = 20$, 1000 counts per spectrum, and various temperatures. Then we fitted these simulated spectra with isothermal models assuming solar abundances and compared the fitted temperatures to the true temperature. The number of successful fits and the relative deviations of the fitted temperatures (T) from the true temperatures (T_0) are shown in Fig. 9.

For $Z = 0.5$ we can find no significant deviations of the fitted temperatures from the true temperatures. The largest systematic deviations occur for $\log T \approx 7.6$, where the temperatures are overestimated by $\lesssim 25\%$. However, it should be noted that this does not exceed the typical uncertainties of the fitted temperatures (see last paragraph).

In the case of an extreme metal under-abundance ($Z = 0.1$), spectra with $\log T \approx 7.0$ cannot be successfully fitted with solar abundance models. For temperatures between $\log T \approx 7.2$ and $\log T \approx 7.6$ a systematic overestimation of the temperature by up to a factor of 2 may occur. However, these deviations are not much larger than the typical uncertainties of the fitted temperatures and restricted to a relatively narrow temperature interval. Furthermore, it should be noted that no significant deviations are found for $\log T \gtrsim 7.6$.

This means that the high maximum temperatures found for many stars in our sample cannot be explained as an artifact caused by assuming wrong abundances. Therefore we conclude that non-solar abundances do not strongly affect the results of our study.

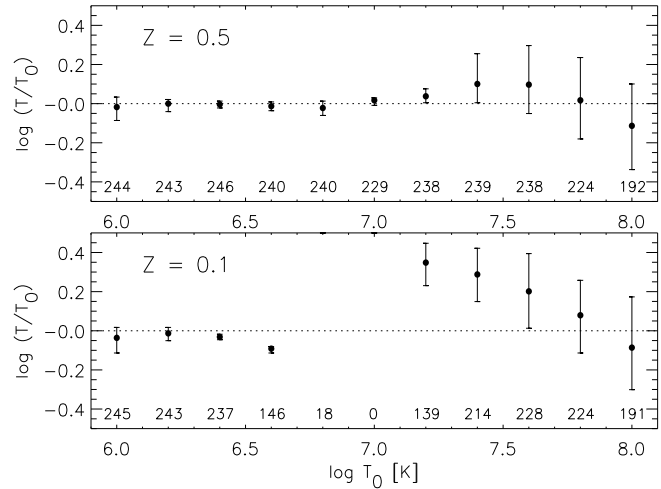


Fig. 9. Relative deviations of temperatures found in fits with solar abundance models to the true temperatures T_0 of simulated spectra with reduced metal abundances. The solid dots show the median of the fitted temperatures, the error bars show the $1\text{-}\sigma$ intervals. The numbers at the bottom of the plots give the number of successful fits. No data are plotted for model parameters where less than half of the 250 simulated spectra could be fitted successfully.

References

- Antiochos, S.K. & Noci, G., 1986, *ApJ* 301, 440
 Basri, G., 1987, *ApJ* 316, 377
 Basri, G., Marcy, G.W. & Valenti, J.A., 1992, *ApJ* 390, 622
 Bouvier, J., 1990, *AJ* 99, 946
 Bouvier, J., 1994, in: *8th Cambridge Workshop on Cool Stars, Stellar System, and the Sun*, ed. J.-P. Caillault, ASP Conference Series Vol 64, p. 151
 Bowyer, S. & Malina, R.F., 1991, in: *Extreme Ultraviolet Astronomy*, eds. S. Bowyer & R.F. Malina, Pergamon Press, New York, p. 397
 Bruner, M.E. & McWriter, R.W.P., 1988, *ApJ* 326, 1002
 Caillault, J.-P., Gagné, M., & Stauffer, J.R., 1994, *ApJ* 432, 386
 Casanova, S., Montmerle, T., Feigelson, E.D., & André, P., 1995, *ApJ* 439, 752
 Dere, K.P. & Mason, H.E., 1993, *Sol. Phys.* 144, 217
 Dorren, J.D. & Guinan, E.F., 1994, *ApJ* 428, 805
 Dorren, J.D., Güdel, M., & Guinan, E.F., 1995, *ApJ* 448, 431
 Doyle, J.G., Mason, H.E., & Vernazza, J.E., 1985, *A&A* 150, 69
 Drake, J.J., 1996, in: *9th Cambridge Workshop on Cool Stars, Stellar System, and the Sun*, eds. R. Pallavicini & A.K. Dupree, ASP Conference Series, in press
 Drake, S.A., Singh, K.P., White, N.E., & Simon, T., 1994, *ApJ* 436, L87
 Drake, J.J., Laming, J.M., & Widing, K.G., 1995, *ApJ* 443, 393
 Drake, J.J., Laming, J.M., & Widing, K.G., 1996a, in: *Astrophysics in the Extreme Ultraviolet*, eds. S. Bowyer & R.F. Malina, Kluwer Academic Publishers, Dordrecht, p. 97
 Drake, S.A., Singh, K.P., & White, N.E., 1996b, in: *Astrophysics in the Extreme Ultraviolet*, eds. S. Bowyer & R.F. Malina, Kluwer Academic Publishers, Dordrecht, p. 147
 Feigelson, E.D., Casanova, S., Montmerle, T., & Guibert, J., 1993, *ApJ* 416, 623
 Fleming, Th.A., Schmitt, J.H.M.M., & Giampapa, M.S., 1995, *ApJ* 450, 401

- Gagné, M. & Caillault, J.-P., 1994, *ApJ* 437, 361
- Gagné, M., Caillault, J.-P., & Stauffer, J.R., 1995a, *ApJ* 445, 280
- Gagné, M., Caillault, J.-P., & Stauffer, J.R., 1995b, *ApJ* 450, 217
- Gauvin, L.S. & Strom, K.M., 1992, *ApJ* 385, 217
- Giampapa, M.S., Rosner, R., Kashyap, V., Fleming, T.A., Schmitt, J.H.M.M., & Bookbinder, J.A., 1996, *ApJ* 463, 707
- Güdel, M., Guinan, E.F., & Skinner, S.L., 1996a, in: *Proc. 'Röntgenstrahlung from the Universe'*, eds. H.U. Zimmermann, J. Trümper, & H.W. Yorke, MPE Report 263, p. 39
- Güdel, M., Guinan, E.F., & Skinner, S.L., 1996b, *A&A*, submitted
- Günther, E.W., 1996, in: *9th Cambridge Workshop on Cool Stars, Stellar System, and the Sun*, eds. R. Pallavicini & A.K. Dupree, ASP Conference Series, in press
- Haisch, B. & Schmitt, J.H.M.M., 1996, *PASP* 108, 113
- Haisch, B., Drake, J.J., Schmitt, J.H.M.M., 1994, *ApJ* 421, L39
- Hara, H., Tsuneta, S., Lemen, J.R., Acton, L.W., & McTiernan, J.M., 1992, *PASJ* 44, L135
- Hempelmann, A., Schmitt, J.H.M.M., Schultz, M., Rüdiger, G., & Stepien, K., 1995, *A&A* 294, 515
- Henoux, J.-C., 1995, *AdSpR* 15, 23
- Herbig, G.H. & Bell, K.R., 1988, *Lick Observatory Bulletin* No. 1111
- Huenemoerder, D.P., Lawson, W.A., & Feigelson, E.D., 1994, *MNRAS* 271, 967
- Johns-Krull, C.M. & Valenti, J.A., 1996, *ApJ* 459, L95
- Maggio, A. & Peres, G., 1996, *A&A*, in press
- Maggio, A., Sciortino, S., Collura, A., & Harnden Jr., F.R., 1995, *A&AS* 10, 573
- Majer, P., Schmitt, J.H.M.M., Golub, L., Harnden, F.R., & Rosner, R., 1986, *ApJ* 300, 360
- Mewe, R., Kaastra, J.S., White, S.M., & Pallavicini, R., 1996, *A&A*, in press
- Meyer, J.-P., 1985, *ApJS* 57, 173
- Micela, G., Sciortino, S., Vaiana, G.S., Schmitt, J.H.M.M., Stern, R.A., & Rosner, R., 1988, *ApJ* 325, 798
- Micela, G., Sciortino, S., Vaiana, G.S., Harnden, F.R., & Schmitt, J.H.M.M., 1990, *ApJ* 348, 557
- Montmerle, T., Koch-Miramond, L., Falgarone, E., & Grindlay, J.E., 1983, *ApJ* 269, 182
- Montmerle, T., Feigelson, E.D., Bouvier, J., & Andre, P., 1993, in: *Protostars and planets III*, eds. E.H. Levy & J.I. Lunine, University of Arizona Press, p. 689
- Morrison, R. & McCammon, D., 1983, *ApJ* 270, 119
- Ottmann, R., 1993, *A&A* 273, 546
- Ottmann, R., 1994, *A&A* 286, L27
- Ottmann, R. & Schmitt, J.H.M.M., 1994, *A&A* 283, 871
- Pallavicini, R., 1989, *A&A Rev.* 1, 177
- Pallavicini, R., Golub, L., Rosner, R., Vaiana, G.S., Ayres, T., & Linsky, J.L., 1981, *ApJ* 248, 279
- Pallavicini, R., Tagliaferri, G. & Stella, L., 1990, *A&A* 228, 403
- Pan, H.C., & Jordan, C., 1995, *MNRAS* 272, 11
- Paresce, F., 1984, *AJ* 89, 1022
- Parker, E.N., 1988, in: *Solar and Stellar Coronal Structure and Dynamics*, ed. R.C. Altrock, *Nat. Solar Obs.*, p. 2
- Patten, B.M. & Simon, T., 1993, *ApJ* 415, L23
- Pfeffermann, E., Briel, U.G., Hippmann, H., et al., 1987, *Proc. SPIE* 733, 519
- Phillips, K.J.H., Pike, C.D., Lang, J., Zarro, D.M., Fludra, A., Watanabe, T., & Takahashi, M., 1995, *AdSpR* 15, 33
- Porter, J.G., Moore, R.L., Reichmann, E.J., Engvold, E., & Harvey, K.L., 1987, *ApJ* 323, 380
- Predehl, P. & Schmitt, J.H.M.M., 1995, *A&A* 293, 889
- Preibisch, Th., Zinnecker, H., & Schmitt, J.H.M.M., 1993, *A&A* 279, L33
- Preibisch, Th. & Neuhäuser, R., 1995, in: *IAU Colloquium 151: Flares and Flashes*, eds. J.Greiner et al., Springer Verlag, p. 212
- Preibisch, Th., Neuhäuser, R., & Alcalá, J.M., 1995, *A&A* 304, L13
- Press, W.H., Flannery, B.P., Teukolsky, S.A. & Vetterling, W.T., 1986, *Numerical recipes*, Cambridge University Press
- Prosser, C.F., Shetrone, M.D., Dasgupta, A., et al., 1995, *PASP* 107, 211
- Raymond, J.C., 1988, in: *Hot Thin Plasmas in Astrophysics*, ed. R. Pallavicini, Kluwer Academic Publishers, p. 3
- Raymond, J.C. & Smith, B.W., 1977, *ApJS* 35, 419
- Robinson, R.D., Carpenter, K.G., Percival, J.W., & Bookbinder, J.A., 1995, *ApJ* 451, 795
- Rosner, R., Tucker, W.H. & Vaiana, G.S., 1978, *ApJ* 220, 643
- Schmitt, J.H.M.M., Collura, A., Sciortino, S., Vaiana, G.S., Harnden, F.R., & Rosner, R., 1990, *ApJ* 365, 704
- Schmitt, J.H.M.M., Fleming, Th.A., & Giampapa, M.S., 1995, *ApJ* 450, 392
- Schrijver, C.J., Mewe, R., van den Oord, G.H.J., & Kaastra, J.S., 1995, *A&A* 302, 438
- Serio, S., Peres, G., Vaiana, G.S., Golub, L., & Rosner, R., 1981, *ApJ* 243, 288
- Singh, K.P., White, N.E., Drake, S.A., 1996, *ApJ* 456, 766
- Smith, M.D., 1994, *A&A* 287, 523
- Stauffer, J.R., 1994, in: *8th Cambridge Workshop on Cool Stars, Stellar System, and the Sun*, ed. J.-P. Caillault, ASP Conference Series Vol 64, p. 163
- Stauffer, J.R., Caillault, J.-P., Gagné, M., Prosser, C.F., & Hartmann, L.W., 1994, *ApJS* 91, 625
- Stern, R.A., Schmitt, J.H.M.M., Pye, J.P., Hodkin, S.T., Stauffer, J.R., & Simon, T., 1994, *ApJ* 427, 808
- Stern, R.A., Lemen, J.R., Schmitt, J.H.M.M., & Pye, J.P., 1995, *ApJ* 444, L45
- Stern, R.A., Schmitt, J.H.M.M., & Kahabka, P.T., 1995, *ApJ* 448, 683
- Trümper, J., 1983, *AdSpR* 2, 241
- Vaiana, G.S. & Rosner, R., 1978, *ARA* 16, 393
- Watanabe, T., 1996, *AdSpR* 17, 239
- Yoshida, T. & Tsuneta, S., 1996, *ApJ* 459, 342
- Zimmermann, H.U., Belloni, T., Izzo, C., Kahabka, P., & Schwentker, O., 1993, *EXSAS User's Guide*, MPE Report 244, Garching